NUCLEAR THEORY, Vol. 32 (2013)
eds. A.I. Georgieva, N. Minkov, Heron Press, Sofia

Nuclear Structure Evolution in Mg Isotopes between Proton and Neutron Drip Lines

M.K. Gaidarov[1], **P. Sarriguren**[2], **A.N. Antonov**[1], **E. Moya de Guerra**[3]

[1]Institute for Nuclear Research and Nuclear Energy, Bulgarian Academy of Sciences, Sofia 1784, Bulgaria

[2]Instituto de Estructura de la Materia, IEM-CSIC, Serrano 123, E-28006 Madrid, Spain

[3]Departamento de Fisica Atomica, Molecular y Nuclear, Facultad de Ciencias Fisicas, Universidad Complutense de Madrid, E-28040 Madrid, Spain

Abstract. A comprehensive study of various ground-state properties of neutron-rich and neutron-deficient Mg isotopes with A=20–36 is performed in the framework of the self-consistent Skyrme-Hartree-Fock plus BCS method. The correlation between the skin thickness and the characteristics related with the density dependence of the nuclear symmetry energy is investigated for the same isotopic chain following the theoretical approach based on the coherent density fluctuation model. The results of the calculations show that the behavior of the nuclear charge radii and the nuclear symmetry energy in the Mg isotopic chain is closely related to the nuclear deformation. A particular attempt is made to understand the most recent signatures for existence of an "island of inversion" at neutron-rich ^{32}Mg nucleus (N=20) from the spectroscopic measurements of its low-lying energy spectrum and the charge rms radii of all magnesium isotopes in the sd shell.

1 Introduction

The study of nuclear structure has advanced on the basis of the shell structure associated with the magic numbers. This study, however, has been carried out predominantly for stable nuclei, which are on or near the β-stability line in the nuclear chart and have been explored experimentally. Advances in measurements of unstable nuclei have provided information on exotic nuclei toward the neutron and proton drip lines. Close to them, a large variety of formerly unknown nuclear configurations has been observed. The magic numbers in such exotic systems can be a quite intriguing issue. New magic numbers appear and some others disappear in moving from stable to exotic nuclei in a rather novel manner due to a particular part of the nucleon-nucleon interaction.

Low-lying states of neutron-rich nuclei around the neutron number N=20 attract a great interest, as the spherical configurations associated with the magic number disappear in the ground states. For ^{32}Mg, from the observed population

of the excited 0_2^+ state (found at 1.058 MeV) in the (t,p) reaction on ^{30}Mg, it is suggested [1] that the 0_2^+ state is a spherical one coexisting with the deformed ground state and that their relative energies are inverted at N=20. Very recently, a next signature of an existence of "island of inversion" has been experimentally tested by measuring the charge radii of all magnesium isotopes in the sd shell at ISOLDE-CERN [2] showing that the borderline of this "island" lies between ^{30}Mg and ^{31}Mg.

Inspired by these new observations, in the present work we aim to perform a systematic study of the nuclear ground-state properties of neutron-rich and neutron-deficient Mg isotopes with A=20–36, such as charge rms radii, two-neutron separation energies, neutron, proton, and charge density distributions, neutron (proton) rms radii and related with them thickness of the neutron (proton) skins. This is done in the framework of the deformed HF+BCS method with Skyrme-type density-dependent effective interactions [3]. The need of information for the symmetry energy in finite nuclei, even theoretically obtained, is a major issue because it allows one to constrain the bulk and surface properties of the nuclear energy-density functionals quite effectively. Therefore, following our recent works [4,5] we analyze the correlation between the skin thickness and the characteristics related to the density dependence of the nuclear symmetry energy for the same isotopic chain. A special attention is paid to the neutron-rich ^{32}Mg nucleus because of the weakening of the shell closure and appearance of the "island of inversion" at N=20.

2 Theoretical Framework

The symmetry energy for asymmetric nuclear matter (ANM) $s^{ANM}(\rho)$ is related to the second derivative of the energy per particle $E(\rho,\delta)$ using its Taylor series expansion in terms of the isospin asymmetry $\delta=(\rho_n-\rho_p)/\rho$, where ρ, ρ_n and ρ_p are the baryon, neutron and proton densities, respectively, (see, e.g., [4–7]):

$$s^{ANM}(\rho)=\frac{1}{2}\left.\frac{\partial^2 E(\rho,\delta)}{\partial\delta^2}\right|_{\delta=0} = a_4+\frac{p_0^{ANM}}{\rho_0^2}(\rho-\rho_0)+\frac{\Delta K^{ANM}}{18\rho_0^2}(\rho-\rho_0)^2+\cdots . \quad (1)$$

In Eq. (1) the parameter a_4 is the symmetry energy at equilibrium ($\rho=\rho_0$). In ANM the pressure p_0^{ANM} and the curvature ΔK^{ANM} are:

$$p_0^{ANM}=\rho_0^2\left.\frac{\partial s^{ANM}(\rho)}{\partial\rho}\right|_{\rho=\rho_0}, \quad (2)$$

$$\Delta K^{ANM}=9\rho_0^2\left.\frac{\partial^2 s^{ANM}(\rho)}{\partial\rho^2}\right|_{\rho=\rho_0}. \quad (3)$$

In Refs. [4,5] we calculated the symmetry energy, the pressure and the curvature for *finite* nuclei applying the coherent density fluctuation model [8, 9]. The

key ingredient element of the calculations is the weight function that in the case of monotonically decreasing local densities ($d\rho(r)/dr \leq 0$) can be obtained using a known density distribution for a given nucleus:

$$|f(x)|^2 = -\frac{1}{\rho_0(x)} \left.\frac{d\rho(r)}{dr}\right|_{r=x}, \tag{4}$$

where $\rho_0(x) = 3A/4\pi x^3$ and with the normalization $\int_0^\infty dx|f(x)|^2 = 1$.

It can be shown in the CDFM that under some approximation the properties of *finite nuclei* can be calculated using the corresponding ones for nuclear matter, folding them with the weight function $|f(x)|^2$. Along this line, in the CDFM the symmetry energy for finite nuclei and related quantities are obtained as infinite superpositions of the corresponding ANM quantities weighted by $|f(x)|^2$:

$$s = \int_0^\infty dx|f(x)|^2 s^{ANM}(x), \tag{5}$$

$$p_0 = \int_0^\infty dx|f(x)|^2 p_0^{ANM}(x), \tag{6}$$

$$\Delta K = \int_0^\infty dx|f(x)|^2 \Delta K^{ANM}(x). \tag{7}$$

The explicit forms of the ANM quantities $s^{ANM}(x)$, $p_0^{ANM}(x)$, and $\Delta K^{ANM}(x)$ in Eqs. (5), (6), and (7) are defined below. They have to be determined within a chosen method for the description of the ANM characteristics. In the present work, as well as in Refs. [4, 5], considering the pieces of nuclear matter with density $\rho_0(x)$, we use for the matrix element $V(x)$ of the nuclear Hamiltonian the corresponding ANM energy from the method of Brueckner *et al.* [10, 11]:

$$V(x) = AV_0(x) + V_C - V_{CO}, \tag{8}$$

where

$$\begin{aligned} V_0(x) = 37.53[&(1+\delta)^{5/3} + (1-\delta)^{5/3}]\rho_0^{2/3}(x) \\ &+ b_1\rho_0(x) + b_2\rho_0^{4/3}(x) + b_3\rho_0^{5/3}(x) \\ &+ \delta^2[b_4\rho_0(x) + b_5\rho_0^{4/3}(x) + b_6\rho_0^{5/3}(x)] \end{aligned} \tag{9}$$

with $b_1 = -741.28$, $b_2 = 1179.89$, $b_3 = -467.54$, $b_4 = 148.26$, $b_5 = 372.84$, and $b_6 = -769.57$. In Eq. (8) $V_0(x)$ is the energy per particle in nuclear matter (in MeV) accounting for the neutron-proton asymmetry, V_C is the Coulomb energy of protons in a flucton, and V_{CO} is the Coulomb exchange energy. Thus, using the Brueckner theory, the symmetry energy $s^{ANM}(x)$ and the related quantities for ANM with density $\rho_0(x)$ (the coefficient a_4 in Eq. (1)) have the forms:

$$s^{ANM}(x) = 41.7\rho_0^{2/3}(x) + b_4\rho_0(x) + b_5\rho_0^{4/3}(x) + b_6\rho_0^{5/3}(x), \tag{10}$$

$$p_0^{ANM}(x) = 27.8\rho_0^{5/3}(x) + b_4\rho_0^2(x) + \frac{4}{3}b_5\rho_0^{7/3}(x) + \frac{5}{3}b_6\rho_0^{8/3}(x), \qquad (11)$$

and

$$\Delta K^{ANM}(x) = -83.4\rho_0^{2/3}(x) + 4b_5\rho_0^{4/3}(x) + 10b_6\rho_0^{5/3}(x). \qquad (12)$$

In our method (see also [4, 5]) Eqs. (10), (11), and (12) are used to calculate the corresponding quantities in finite nuclei s, p_0, and ΔK from Eqs. (5), (6), and (7), respectively. We note that in the limit case when $\rho(r) = \rho_0\Theta(R - r)$ and $|f(x)|^2$ becomes a δ function [see Eq. (4)], Eq. (5) reduces to $s^{ANM}(\rho_0) = a_4$.

The neutron skin thickness is usually estimated as the difference of the rms radii of neutrons and protons:

$$\Delta R = < r_{\rm n}^2 >^{1/2} - < r_{\rm p}^2 >^{1/2} . \qquad (13)$$

In our calculations the following Skyrme force parametrizations are used: SLy4, SGII, and Sk3 (see, e.g., [4]). Also, we use the proton and neutron densities obtained from self-consistent deformed Hartree-Fock calculations with density-dependent Skyrme interactions [12] and accounting for pairing correlations.

3 Results of Calculations and Discussion

The nuclear deformation plays an important role to determine the charge and matter radius of the neutron-rich nuclei, in particular for the description of the structure of the Mg isotopes [13–15]. The evolution of the quadrupole parameter $\beta = \sqrt{\pi/5}Q/(A\langle r^2\rangle^{1/2})$ (Q being the mass quadrupole moment and $\langle r^2\rangle^{1/2}$ the nucleus rms radius) as a function of the mass number A is presented in Figure 1. First, as expected, the semi-magic ^{20}Mg isotope (N=8) is spherical, while the open-shell Mg isotopes within this chain possess two equilibrium shapes, oblate and prolate. Due to the conjunction of the N=Z=12 deformed shell effects, the nucleus ^{24}Mg is the most deformed of the isotopic chain. Most of the deformed isotopes turn out prolate with the exception of ^{26,27}Mg and ^{29,31}Mg which have an oblate shape. Our HF+BCS calculations lead to a spherical minimum in the deformation energy curve for the semi-magic ^{32}Mg isotope thus showing that the magic number N=20 exists for the ground-state of ^{32}Mg in the mean-field theories [15]. Also, it is seen from Figure 1 that the prolate deformation grows with the increase of the neutron number for $^{32-36}$Mg. We find almost identical values of the quadrupole parameter β with the three Skyrme parametrizations.

The charge radius is related to the deformation and the isotope shifts of charge radii can be used to investigate the deformations in the isotopic chains. Our results for the squared charge radii differences in Mg isotopes obtained from three different Skyrme forces, SLy4, SGII and Sk3, are shown in Figure 2. We compare them with the experimental data, taking the radius of ^{26}Mg as the reference [2]. In general, different Skyrme forces do not differ much in their predictions of charge rms radii of magnesium spanning the complete sd shell. The

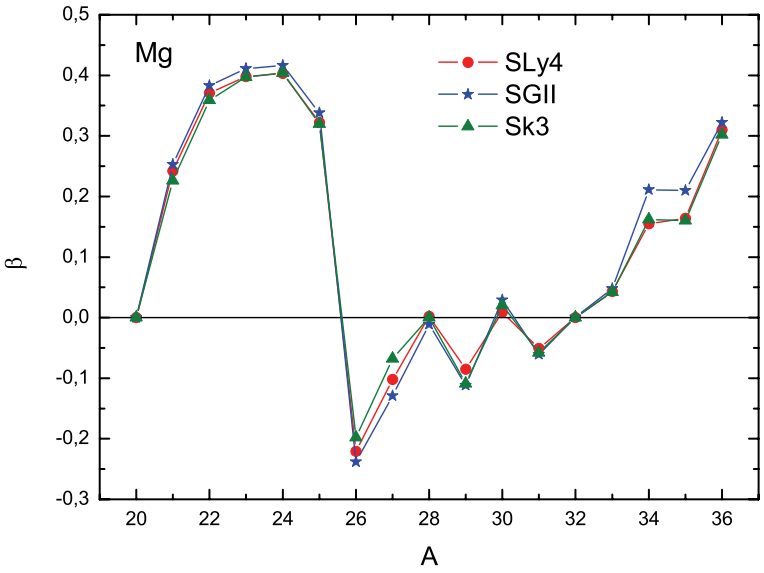

Figure 1. The quadrupole parameter β as a function of the mass number A for Mg isotopes (A=20-36) in the cases of SLy4, SGII, and Sk3 forces.

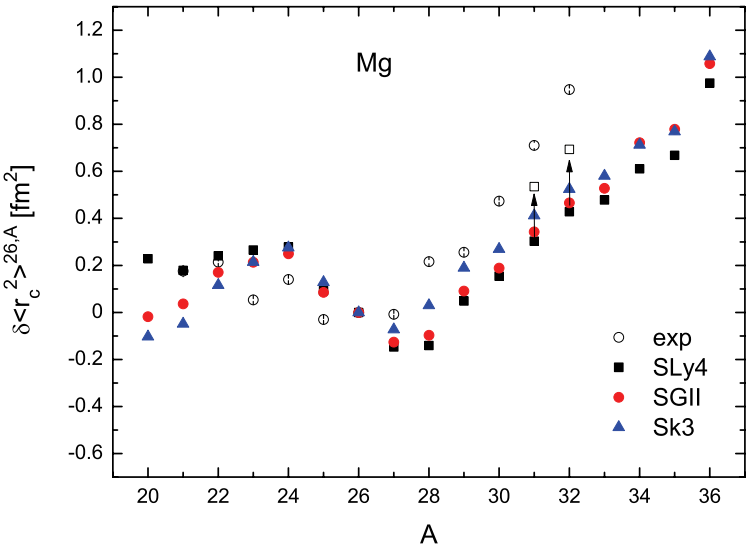

Figure 2. Theoretical (with different Skyrme forces) and experimental [2] isotope shifts $\delta\langle r_c^2\rangle$ of magnesium isotopes relative to ^{26}Mg.

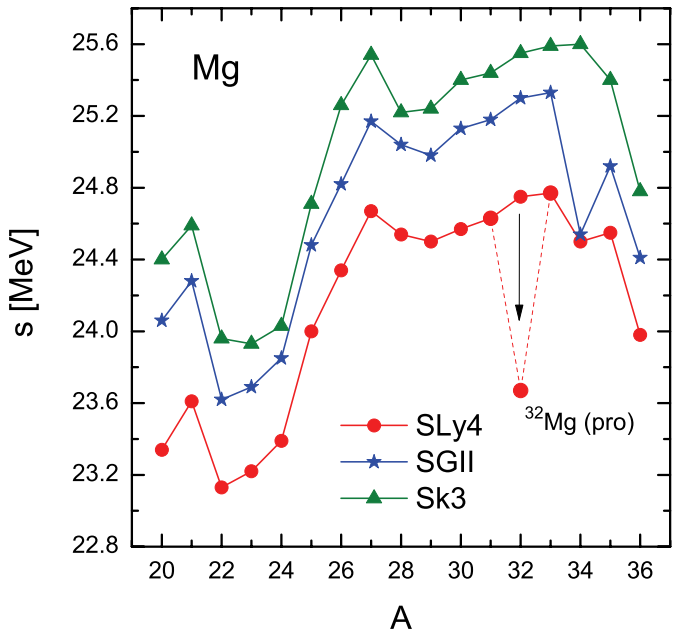

Figure 3. The symmetry energies s for Mg isotopes (A=20-36) calculated with SLy4, SGII, and Sk3 forces.

trend of the behavior of the experimental points and theoretical values strongly corresponds to the neutron shell structure. For $^{21-26}$Mg isotopes the charge distribution is compressed due to the filling of the $d_{5/2}$ orbital and the charge radii do not fluctuate too much. The addition of two neutrons on either $s_{1/2}$ or $d_{3/2}$ in the range $^{28-30}$Mg results in a fast increase of the radius. Finally, for isotopes beyond ^{30}Mg, where the "island of inversion" does exist in terms of the rms charge radius [2], the theoretical results underestimate the experimental points. Obviously, an additional treatment is needed to understand in greater detail this specific region. We note the intermediate position of ^{27}Mg, where a minimum is observed in Figure 2, since one of the neutron added to ^{25}Mg fills the last $d_{5/2}$ hole and another populates the $s_{1/2}$ subshell.

The results for the symmetry energy s [Eq. (5)] as a function of the mass number A for the whole Mg isotopic chain (A=20-36) are presented in Figure 3. The SGII and Sk3 forces yield values of s comparable with each other that lie above the corresponding symmetry energy values when using SLy4 set. Although the values of s slightly vary within the Mg isotopic chain (23–26 MeV) when using different Skyrme forces, the curves presented in Figure 3 exhibit the same trend. We show in Figure 4 the correlation of the neutron-skin thickness ΔR [Eq. (13)] of Mg isotopes with the s and p_0 parameters extracted from the density dependence of the symmetry energy around the saturation density. In

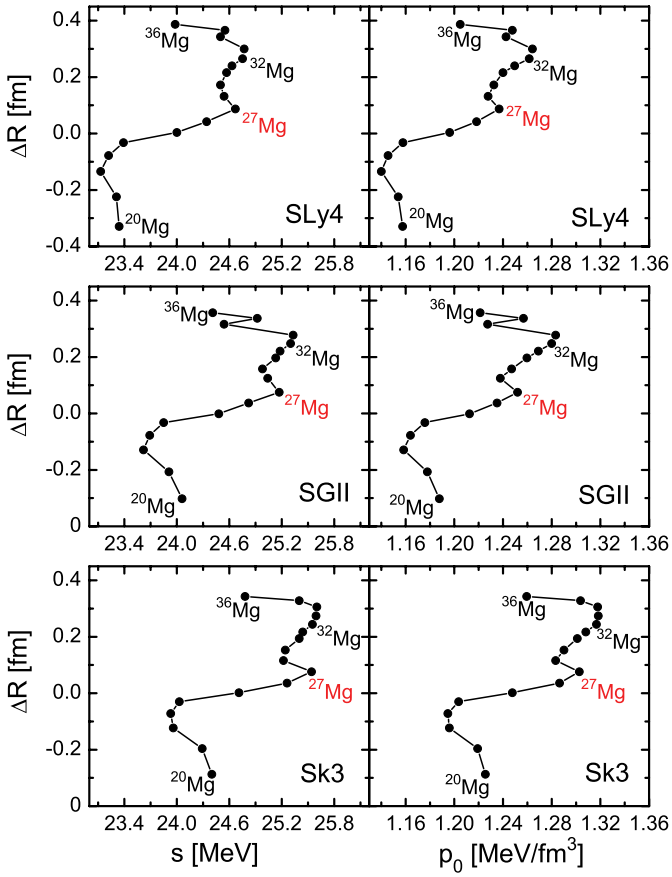

Figure 4. HF + BCS neutron skin thicknesses ΔR for Mg isotopes as a function of the symmetry energy s and the pressure p_0 calculated with SLy4, SGII, and Sk3 forces.

contrast to the results obtained in Refs. [4, 5], there is no linear correlation observed for the Mg isotopic chain. Additionally, we find the same peculiarity at A=27 from Figure 2 for the case of the charge radii just reflecting the transition regions between different nuclear shapes of Mg isotopes in the considered chain and a small change in the behaviour for nuclei heavier than ^{32}Mg, as well. In our opinion, it is useful to search for possible indications of an "island of inversion" around N=20 revealed also by the symmetry energy.

Along this line, to understand better the specific neutron shell-model structure leading to a concept of an "island of inversion" two configurations for ^{32}Mg are displayed in Figure 5: the closed-shell configuration and the one consisting of two neutrons excited from the $1d_{3/2}$ and $2s_{1/2}$ orbitals into the $1f_{7/2}$ and $2p_{3/2}$ orbitals across the $N = 20$ shell gap, making a two-particle, two-hole

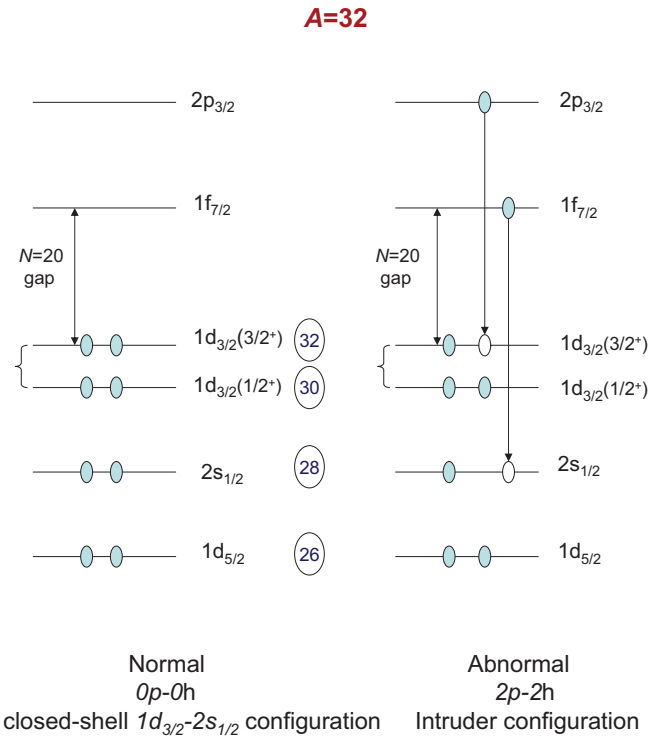

Figure 5. The closed-shell and intruder configurations for ^{32}Mg nucleus.

state. It is well presumed that namely this promotion of a neutron pair results in deformed $2p$-$2h$ intruder ground state from the fp shell which competes with the excited (at 1.06 MeV) spherical normal neutron $0p$-$0h$ state of the sd shell.

As is well known, the spin-orbit interaction and the pairing correlations have influence on the deformation of nuclei. Therefore, we perform additional calculations for the ^{32}Mg nucleus by increasing the spin-orbit strength of the SLy4 effective interaction with 20%. As a result, we find strong prolate deformation for the intruder configuration (β=0.38) and further increase of the charge radius. The latter is illustrated in Figure 6, where the result of the same procedure applied to ^{31}Mg nucleus is also shown. Such a modified calculation causes an increase of the isotope shifts toward the experimentally extracted values for both nuclei indicated in Figure 2 and a significant change in the nuclear symmetry energy of ^{32}Mg (Figure 3). It can be seen from Figure 6 that the comparison between the new values that are very close to the experimental data [2] and the previously obtained values of the charge radii of ^{31,32}Mg isotopes can define a region associated with the "island of inversion" which is not seen in the HF+BCS theoretical method by using the original Skyrme force fitted to stable nuclei.

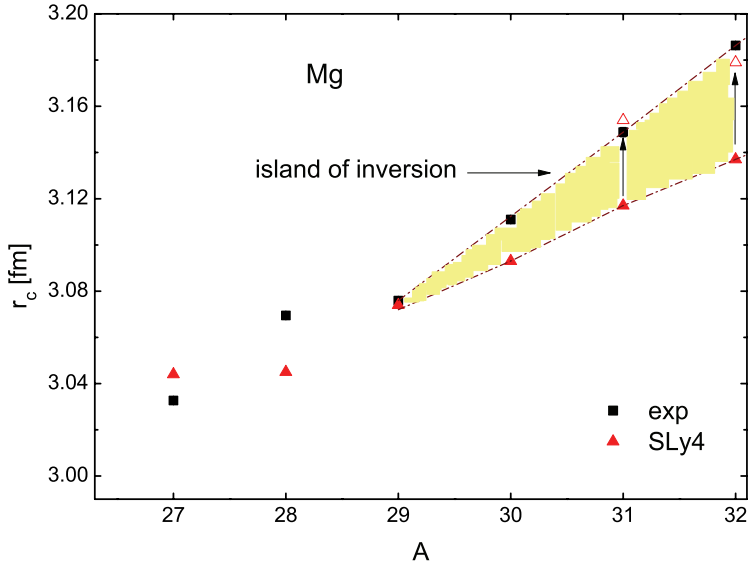

Figure 6. Theoretical (with the SLy4 Skyrme force) and experimental [2] rms charge radii r_c of Mg isotopes in the range A=27–32. The open red triangles represent the calculated values of r_c when the spin-orbit strength of the effective interaction is increased by 20%.

4 Conclusions

In this work, a theoretical approach to the nuclear many-body problem combining the deformed HF+BCS method with Skyrme-type density-dependent effective interactions [3] and the coherent density fluctuation model [8, 9] has been used to study nuclear properties of Mg isotopes from the proton-drip-line nucleus ^{20}Mg to ^{36}Mg being very closed to the neutron drip line. Three Skyrme parametrizations were involved in the calculations: SLy4, SGII, and Sk3. We have demonstrated the capability of CDFM to be applied as an alternative way to make a transition *from the properties of nuclear matter to the properties of finite nuclei* investigating the nuclear symmetry energy s and the neutron pressure p_0. This has been carried out on the base of the Brueckner energy-density functional for infinite nuclear matter.

The deformation energy curves illustrate a transition from the spherical ^{20}Mg (N=8) to the prolate shape of ^{36}Mg (N=24) through prolate (N=10,12), oblate (N=14), with shallow spherical minima (N=16,18) and again spherical ^{32}Mg (N=20). The neutron densities are lower that the proton ones when $N < Z$, similar when N=Z, and larger when $N > Z$, as expected. There is also a strong increase of the neutron densities at ^{27,28}Mg (N=15,16) that occurs when the neutrons occupy the $s_{1/2}$ shell. For heavier isotopes the increase is very smooth again. The charge radii follow qualitatively the trend observed in the experi-

ment with minima around A=27, several jumps below and a smooth increase above. The correlation between the neutron skin thickness ΔR and the symmetry energy s and neutron pressure p_0 shows up the same peculiarity at A=27 just reflecting the transition regions between different nuclear shapes of Mg isotopes in the considered chain. The values of the symmetry energy s vary roughly between 23 and 26 MeV being larger for Sk3 force and smaller for SLy4 force and in between for the case of the SGII effective interaction.

Concluding, we would like to note that further study is necessary to prove theoretically the existence of an "island of inversion" probed by the REX-ISOLDE experiment. In particular, it is worth to perform calculations by including effects of tensor and three-body forces and exploring novel energy density functionals.

References

[1] K. Wimmer *et al.*, *Phys. Rev. Lett.* **105** (2010) 252501.

[2] D. T. Yordanov *et al.*, *Phys. Rev. Lett.* **108** (2012) 042504.

[3] D. Vautherin, *Phys. Rev. C* **7** (1973) 296-316.

[4] M. K. Gaidarov, A. N. Antonov, P. Sarriguren, and E. Moya de Guerra, *Phys. Rev. C* **84** (2011) 034316.

[5] M. K. Gaidarov, A. N. Antonov, P. Sarriguren, and E. Moya de Guerra, *Phys. Rev. C* **85** (2012) 064319.

[6] A. E. L. Dieperink, Y. Dewulf, D. Van Neck, M. Waroquier, and V. Rodin, *Phys. Rev. C* **68** (2003) 064307.

[7] Lie-Wen Chen, *Phys. Rev. C* **83** (2011) 044308.

[8] A. N. Antonov, V. A. Nikolaev, and I. Zh. Petkov, *Bulg. J. Phys.* **6** (1979) 151; *Z. Phys. A* **297** (1980) 257; *ibid* **304** (1982) 239; *Nuovo Cimento A* **86** (1985) 23; A. N. Antonov *et al.*, *ibid* **102** (1989) 1701; A. N. Antonov, D. N. Kadrev, and P. E. Hodgson, *Phys. Rev. C* **50** (1994) 164-167.

[9] A. N. Antonov, P. E. Hodgson, and I. Zh. Petkov, *Nucleon Momentum and Density Distributions in Nuclei* (Clarendon Press, Oxford, 1988); *Nucleon Correlations in Nuclei* (Springer-Verlag, Berlin-Heidelberg-New York, 1993).

[10] K. A. Brueckner, J. R. Buchler, S. Jorna, and R. J. Lombard, *Phys. Rev.* **171** (1968) 1188-1195.

[11] K. A. Brueckner, J. R. Buchler, R. C. Clark, and R. J. Lombard, *Phys. Rev.* **181** (1969) 1543-1551.

[12] E. Moya de Guerra, P. Sarriguren, J. A. Caballero, M. Casas and D. W. L. Sprung, *Nucl. Phys. A* **529** (1991) 68-94.

[13] W. Horiuchi, T. Inakura, T. Nakatsukasa, and Y. Suzuki, *Phys. Rev. C* **86** (2012) 024614.

[14] J. Terasaki, H. Flocard, P.-H. Heenen, and P. Bonche, *APH N.S., Heavy Ion Physics* **6** (1997) 201-204.

[15] Z. Ren, Z. Y. Zhu, Y. H. Cai, and G. Xu, *Phys. Lett. B* **380** (1996) 241-246.